JOURNAL OF APPLIED PHYSICS VOLUME 87, NUMBER 10 15 MAY 2000

Comparison of linewidth enhancement factors in midinfrared active region materials

J. T. Olesberg, Michael E. Flatté,[a] and Thomas F. Boggess
Department of Physics and Astronomy and the Optical Science and Technology Center, The University of Iowa, Iowa City, Iowa 52242

(Received 21 January 2000; accepted for publication 28 January 2000)

We report calculations of the linewidth enhancement factor for five midinfrared active region materials. The linewidth enhancement factors for two type-I quantum wells based on InAsSb are 2.5 and 5.4, which represent a reduction of up to a factor of 2.6 with respect to bulk $InAs_{0.91}Sb_{0.09}$. However, active region materials based on the type-II, InAs/GaInSb system have linewidth enhancement factors near 1.0, which is a factor of 2–5 reduction compared to the type-I quantum wells. The reduction of the linewidth enhancement factor is associated with both a reduction of the mismatch between the conduction and valence band densities of states and the presence of conduction band dispersion. We describe an additional optimization that is possible in the type-II materials: Carefully placed intersubband absorption features can be used to further reduce the linewidth enhancement factor. We show that linewidth enhancement values as low as 0.3 can be obtained in the type-II superlattices when fabricated into a distributed feedback structure. © *2000 American Institute of Physics.* [S0021-8979(00)07009-2]

I. INTRODUCTION

Many of the potential applications for midinfrared semiconductor lasers, in particular those involving molecular spectroscopy and remote sensing, require coherent sources with narrow linewidths. Spectral purity in a semiconductor laser is degraded by the coupling between phase and amplitude noise such that the linewidth is broadened beyond the Schawlow–Townes limit according to[1]

$$\Delta v = \Delta v_0 (1 + \alpha_{\mathrm{lwe}}^2), \tag{1}$$

where Δv_0 is the Schawlow–Townes linewidth and α_{lwe} is the linewidth enhancement factor. The linewidth enhancement factor is also a measure of the likelihood of formation of optical filaments. At high powers, optical filamentation can lead to catastrophic facet damage in the localized optical fields. Devices with small linewidth enhancement factors have the capability of producing larger output powers without facet damage.

The linewidth enhancement factor (α_{lwe}) is defined as the ratio of the density derivative of the real (χ_r) and imaginary (χ_i) parts of the complex susceptibility. However, when the fractional change in the index of refraction is small compared to the fractional change of the absorption coefficient, the linewidth enhancement factor can be written in terms of the density derivatives of the index of refraction (n) and the net gain (γ_{net}),

$$\alpha_{\mathrm{lwe}}(\omega) = \frac{d\chi_r(\omega)/dN}{d\chi_i(\omega)/dN} \approx -\frac{4\pi}{\lambda} \frac{dn(\omega)/dN}{d\gamma_{\mathrm{net}}(\omega)/dN}, \tag{2}$$

where N is the carrier density and ω is the lasing frequency. The net gain, γ_{net}, differs from the fundamental gain due to the presence of intersubband absorption, which can be significant in midinfrared materials. Because dn/dN can be related to the differential gain spectrum by a Kramers–Krönig transformation, the linewidth enhancement factor can be written entirely in terms of the differential gain spectrum

$$\alpha_{\mathrm{lwe}}(\omega) = \frac{2\omega}{\pi} \frac{\int_0^\infty \left(\frac{d\gamma_{\mathrm{net}}(\omega')/dN}{\omega'^2 - \omega^2} \right) d\omega'}{d\gamma_{\mathrm{net}}(\omega)/dN}, \tag{3}$$

or, equivalently,

$$\alpha_{\mathrm{lwe}}(\omega) = \frac{2\omega}{\pi} \int_0^\infty \frac{\left[\frac{d\gamma_{\mathrm{net}}(\omega')/dN}{d\gamma_{\mathrm{net}}(\omega)/dN} \right]}{\omega'^2 - \omega^2} d\omega'. \tag{4}$$

The quantity in square braces in Eq. (4) is the differential gain spectrum *relative* to the magnitude of the differential gain at the lasing wavelength. When written in this form, the linewidth enhancement factor is a function only of the shape of the relative differential gain spectrum. Thus, we can compare material systems of comparable band gaps using their relative differential gain spectra.

Whereas dn/dN (and hence, α_{lwe}) vanishes near the peak of the differential gain spectrum due to the symmetry of the Kramers–Krönig transform, lasers typically operate at the frequency of the peak of the gain spectrum. In interband semiconductor lasers, as contrasted with atomic-like lasers, the peak of the differential gain is shifted away from the peak of the gain due to the opposite curvature of the conduction and valence bands. This shift is increased by any imbalance between conduction and valence band densities of states.[2,3] Because of this, semiconductor lasers typically have

[a]Electronic mail: michael-flatte@uiowa.edu

 © 2000 American Institute of Physics

Downloaded 19 Jan 2005 to 128.255.34.225. Redistribution subject to AIP license or copyright, see http://jap.aip.org/jap/copyright.jsp

linewidth enhancement factors significantly different from zero. Typical values for near-infrared semiconductor lasers range from 2 to 6.[4,5]

Three primary strategies have been employed for reducing the linewidth enhancement factor in near-infrared lasers. The first is to reduce the imbalance between the conduction and valence band densities of states through the use of strain and quantum confinement.[2,6] Reducing the density of states imbalance increases the differential gain at the lasing energy and decreases the width of the differential gain spectrum. The second strategy is to *p* dope the active region, which helps to offset the density of states imbalance.[2,3,6] Third, a distributed feedback grating (DFB) can be used to detune the lasing energy from the peak of the gain towards the peak of the differential gain.[3,7] The amount of detuning that can be used is limited by the range of energies over which there is positive gain. When the peak of the differential gain spectrum lies in the region of positive gain, it is possible to reduce the linewidth enhancement factor to near zero.

The situation is more challenging in the midinfrared since the conduction band effective mass (of a bulk material) decreases roughly proportionally with the band gap, increasing the density of states imbalance. In addition, *p* doping the active region aggravates existing problems with Auger recombination. Thus, producing semiconductor lasers with small linewidth enhancement factors requires careful attention to the problem of density of states mismatch. There have been relatively few reports of linewidth enhancement values for wavelengths beyond 1.55 μm. Meyer *et al.* report calculated values of 1.7 and 4.2 for early midinfrared type-II quantum wells and superlattices at 300 K.[8] Vurgaftman and Meyer have reported a calculated value of 1.1 for the type-II quantum well of Ref. 8 at a temperature of 100 K.[9] Recently, Anson *et al.* reported measurements of small linewidth enhancement factors (<1.0) in a 4 μm type-II superlattice at room temperature.[10] Intersubband quantum cascade lasers are expected to have ultralow linewidth enhancement factors (<0.1) due to the extremely narrow joint density of states characteristic of atomic-like systems.[11]

Here we report calculations of the linewidth enhancement factor at room temperature in a selection of midinfrared active region materials. The linewidth enhancement factor is correlated with three features of the electronic structure: Conduction and valence band density of states balancing, conduction band dispersion, and judiciously placed intersubband absorption features. Calculations were performed on a 4.2 μm strained 150 Å InAsSb/300 Å AlInAsSb quantum well structure,[12] a 4.4 μm strained 80 Å InAsSb/80 Å InAsP quantum well structure,[13] a 4.0 μm 15 Å InAs/25Å $Ga_{0.60}In_{0.40}Sb$/15 Å InAs/39 Å $Al_{0.30}Ga_{0.42}In_{0.28}As_{0.50}Sb_{0.50}$ superlattice,[14,15] and a 4.1 μm 21 Å InAs/31 Å $Ga_{0.75}In_{0.25}Sb$/21 Å InAs/43 Å AlSb superlattice.[16] Bulk $InAs_{0.91}Sb_{0.09}$ (lattice matched to GaSb) is included as a reference. Although the linewidth enhancement factor of a real device is affected by the optical cavity,[4,17] the value is dominated by the inherent linewidth enhancement factor of the active region material. Comparison of the linewidth enhancement factor of the different materials allows for the evaluation of these materials as active regions for either spectrally pure or high-power applications.

II. THEORY

The optical properties of the materials were calculated using a superlattice **K·p** formalism with a 14 bulk band basis. This method is an extension of the eight-band **K·p** formalism that has been used previously to calculate the optical properties of a variety of midinfrared materials.[14] Excellent agreement has been seen between a variety of theoretical calculations and experimental measurements.[18] Gain and intersubband absorption spectra were calculated for transverse electric polarization as a function of carrier density using the highly nonparabolic band structure and momentum-dependent matrix elements. A Kramers–Krönig transformation of the change in absorption spectra for each density was performed to obtain the nonlinear change in the index of refraction. The density dependence of these calculations provide the differential gain and differential index. The linewidth enhancement factor was then calculated from Eq. (2).

Strictly, the Kramers–Krönig transformation should be applied over the entire energy spectrum, whereas we use a finite energy range (transition energies up to $\sim$0.8 eV). However, calculating the *change* in index from the *change* in absorption spectrum is a very different problem than calculating the *index of refraction* from the *absorption* spectrum. The index of refraction is dominated by the magnitude of the absorption spectrum at Van Hove singularities away from zone center, but the change in absorption spectra is only nonzero where the nonequilibrium carriers are (near zone center for the direct gap materials discussed here). We can approximate the effect of using a finite energy range in our calculations by repeating the calculations using a substantially larger energy range. From this procedure, we estimate the error introduced by the use of a finite energy range in the calculation of the change in index spectrum at the expected lasing energy to be less than 10%.

III. LINEWIDTH ENHANCEMENT FACTORS FOR MIDINFRARED MATERIALS

The results of our calculations of linewidth enhancement factors are listed in Table I. In order to facilitate the comparison of different material systems, we focus on the relative differential gain spectrum of Eq. (4). Plots of the gain, relative differential gain, and linewidth enhancement factor are shown in Fig. 1 as a function of transition energy for four of the five systems considered (the curves for system IV are similar to those of system V). These parameters are calculated for the carrier density at which the linewidth enhancement factor at the peak of the gain spectrum takes on its minimum value. By examining Fig. 1 we can track the change of behavior from system I [Fig. 1(a)], which is a bulk system, through system II [Fig. 1(b)] and system III [Fig. 1(c)], which are quantum wells with increasing levels of confinement, to system V [Fig. 1(d)], which is a type-II superlattice with very large band offsets.

Bulk InAsSb has the largest linewidth enhancement factor of all of the systems considered. The large linewidth en-

Downloaded 19 Jan 2005 to 128.255.34.225. Redistribution subject to AIP license or copyright, see http://jap.aip.org/jap/copyright.jsp

TABLE I. Calculated values of the linewidth enhancement factor for five midinfrared active region materials at room temperature. E_g is the band gap, $\alpha_{\rm lwe}$ is the linewidth enhancement factor, ρ_v/ρ_c is a measure of the ratio of the valence to conduction band densities of states, $d\gamma_{\rm net}/dN$ is the differential gain at the peak of the gain spectrum, and $\Delta E_{\rm CB}$ is the miniband width of the lowest conduction subband.

	System	E_g (μm)	$\alpha_{\rm lwe}$ at $\gamma_{\rm net}^{\rm max}$	$\alpha_{\rm lwe}$ $\gamma_{\rm net}>50\ {\rm cm}^{-1}$	ρ_v/ρ_c	$d\gamma/dN$ ($\times 10^{-16}\ {\rm cm}^2$)	$\Delta E_{\rm CB}$ (meV)
	Bulk materials						
I	$InAs_{0.91}Sb_{0.09}$	4.2	6.5	1.8	25.7	3.5	bulk
	Type-I quantum wells						
II	InAsSb/AlInAsSb	4.2	5.4	2.0	9.9	4.8	0.3
III	InAsSb/InAsP	4.4	2.5	1.7	7.6	13.9	21.2
	Type-II superlattices						
IV	InAs/GaInSb/InAs/AlSb	4.1	1.1	0.4	2.0	33.6	2.5
V	InAs/GaInSb/InAs/AlGaInAsSb	4.0	0.9	0.3	2.3	27.0	36.2

hancement factor is fundamentally a consequence of the significant imbalance between the conduction and valence band densities of states. Density of states mismatch leads to a large linewidth enhancement factor through two processes. First, significant imbalance between the densities of states reduces the differential gain near the band edge by decreasing the hole occupation function at the valence band edge. Second, density of states imbalance broadens the differential gain spectrum. The peak of the differential gain spectrum will occur roughly at a transition energy of $E_g+E_{\rm Fc}$, where E_g is the band gap and $E_{\rm Fc}$ is the conduction band Fermi energy measured from the conduction band minima.[3] When the density of states of the valence band is significantly larger than that of the conduction band, $E_{\rm Fc}$ becomes increasingly large.

The imbalance between the conduction and valence densities of states can be quantified using the ratio of the valence and conduction band-edge Fermi occupation functions at a density where the sum of the Fermi functions is 1.0 (which is a minimal condition for gain).[19] This quantity is a measure of the contribution to inversion from the valence and conduction bands. A system with ideal balancing of the densities of states would have a ratio of 1.0. Using this measure, the density of states imbalance for bulk InAsSb is 25.7. Calculated values are shown in Table I for all of the materials.

System II is a compressively strained quantum well with small band offsets for both the electrons (90 meV) and holes (72 meV). The quantum confinement and compressive strain reduce the density of states imbalance to 9.9 by splitting the heavy and light valence subbands. However, the band offsets are not large enough to significantly improve the differential gain, so the linewidth enhancement factor is only slightly smaller than that of bulk InAsSb.

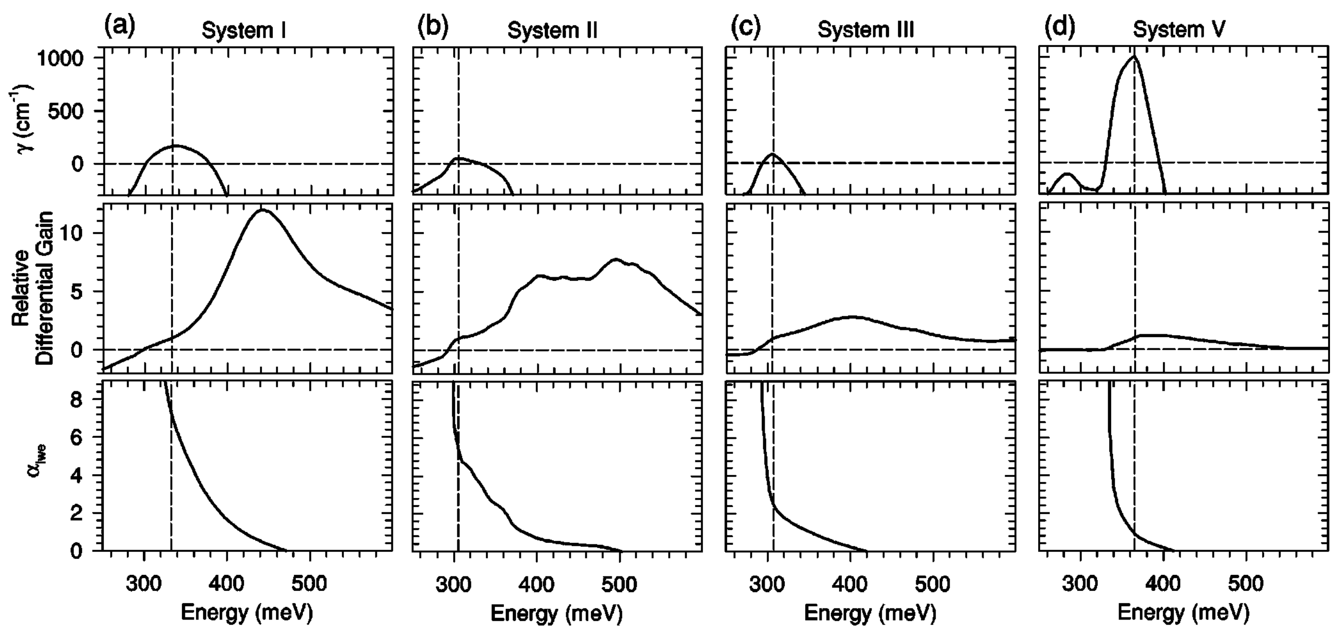

FIG. 1. Gain, relative differential gain, and linewidth enhancement factor as a function of transition energy for (a) system I, bulk $InAs_{0.91}Sb_{0.09}$, (b) system II, an InAsSb/AlInAsSb quantum well, (c) system III, an InAsSb/InAsP quantum well, and (d) system V, a type-II superlattice. The curves for each system are calculated for the carrier density at which the linewidth enhancement factor at the peak of the gain spectrum is a minimum. The vertical dashed lines are the energy of the peak of the gain spectrum.

Downloaded 19 Jan 2005 to 128.255.34.225. Redistribution subject to AIP license or copyright, see http://jap.aip.org/jap/copyright.jsp

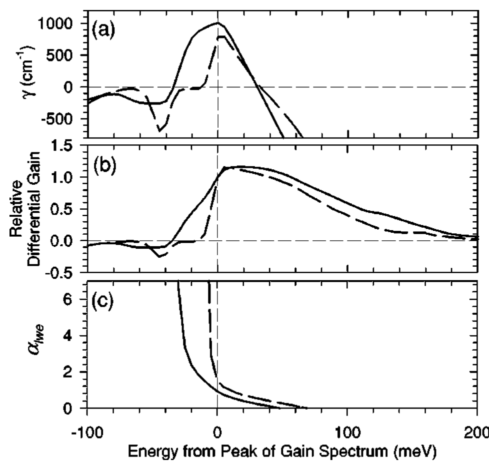

FIG. 2. (a) Gain, (b) relative differential gain, and (c) linewidth enhancement factor spectra for systems IV (dashed line) and V (solid line) as a function of the energy from the peak of the gain spectrum (vertical dashed line).

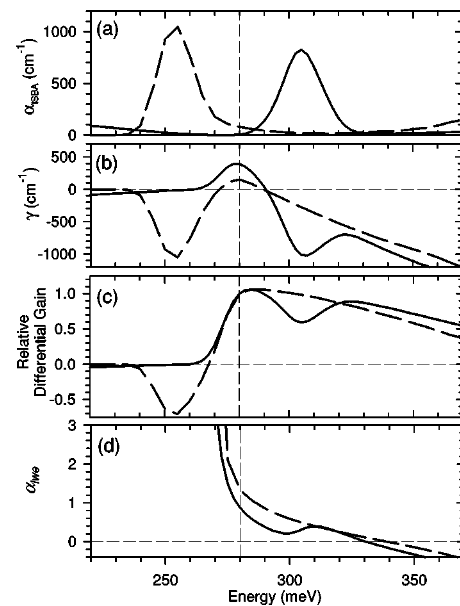

FIG. 3. Placement of intersubband absorption features can be used to reduce the linewidth enhancement factor in type-II superlattices. (a) Intersubband absorption, (b) gain, and (c) relative differential gain, and (d) linewidth enhancement factor spectra for an optimized (solid) and a deoptimized (dashed) four-layer superlattice. The optimized superlattice is 30 Å $Ga_{0.55}In_{0.45}Sb$/18 Å InAs/65 Å $Al_{0.30}Ga_{0.42}In_{0.28}As_{0.50}Sb_{0.50}$; the deoptimized structure is 38 Å $Ga_{0.75}In_{0.25}Sb$/20 Å InAs/65 Å $Al_{0.30}Ga_{0.42}In_{0.28}As_{0.50}Sb_{0.50}$. The vertical dashed line is the energy of the peak of the gain spectrum for both structures.

System III is a multiple quantum well structure with a narrower well, twice the electron and hole confinement, and twice the compressive strain of system II. Because of this, the differential gain at the peak of the gain spectrum ($13.9 \times 10^{-16}\,\mathrm{cm}^2$) is significantly larger than either systems I or II. Thus, the overall magnitude of the relative differential gain at high energies is smaller, reducing the linewidth enhancement factor.

One of the main advantages of the type-II InAs/GaInSb material system is the large band offsets (>0.5 eV) possible in both the conduction and valence bands. In addition, because the valence band well is typically very thin (~20–30 Å), it is possible to incorporate much larger strains (~2.5%) than in the thicker type-I quantum wells. The additional strain and quantum confinement make it possible to design materials with a density of states mismatch that is more than a factor of three smaller than either of the type-I quantum wells. It is this same improvement in the balancing of the density of states that makes the type-II superlattices attractive for low threshold operation.[14] For system V, the differential gain ($27 \times 10^{-16}\,\mathrm{cm}^2$) is more than twice that of system III. In addition, the relative differential gain spectrum is significantly narrower than the bulk and type-I systems.

Within each type of structure (type I or type II), those with larger conduction band dispersion (listed in Table I) have smaller linewidth enhancement factors. The presence of dispersion in the conduction band shifts the peak of the gain spectrum (and hence, the lasing energy) from the band edge to an energy roughly the miniband width above the band edge. The region of positive differential gain between the band edge and the gain spectrum peak reduces the density dependence of the index of refraction and the value of the linewidth enhancement factor at the peak of the gain spectrum. The impact of dispersion in the conduction band on the threshold carrier density of a laser is not substantial, however, if the miniband width is comparable to or smaller than the thermal energy ($k_B T$).

The advantage of conduction band dispersion can be seen in a comparison of systems IV and V. Because system V uses a quinternary alloy as the superlattice barrier layer rather than the much wider band gap AlSb, there is a slight coupling between adjacent periods of the superlattice, which results in 36 meV of dispersion in the conduction band. The impact on the gain, relative differential gain spectrum, and the linewidth enhancement factor can be seen in Fig. 2 as a function of energy from the peak of the gain spectrum. The gain spectrum of system V (solid line) is significantly broader than that of system IV (dashed line) because of the dispersion in the conduction band. The broadening of the gain spectrum at energies below the peak of the gain spectrum results in a broadening of the relative differential gain spectrum. The region of positive differential gain below the peak gain energy reduces the resulting linewidth enhancement factor, in spite of the fact that the differential gain spectrum for system V is broader at energies above the peak gain.

An additional optimization can be used to reduce the linewidth enhancement factor in the type-II superlattices. Intersubband absorption features in these superlattices are relatively sharp due to the highly structured nature of the valence subbands. It is possible to adjust the energy of the subbands by modifying the layer thicknesses and alloy compositions in such a way as to place a large absorptive feature above the peak of the gain spectrum. The presence of this large density-dependent absorption feature just above the lasing energy will reduce the density dependence of the index of refraction at the lasing energy without reducing the differential gain, thereby reducing the linewidth enhancement factor. An example of this is shown in Fig. 3 for two 4.5 μm type-II

Downloaded 19 Jan 2005 to 128.255.34.225. Redistribution subject to AIP license or copyright, see http://jap.aip.org/jap/copyright.jsp

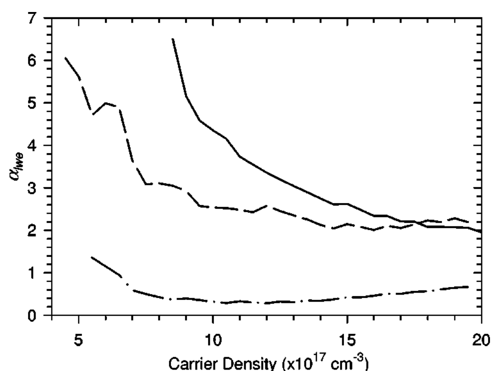

FIG. 4. Minimum linewidth enhancement factor at any energy with greater than 50 cm^{-1} of gain for bulk InAsSb (system I, solid line), a type-I quantum well (system II, dashed line), and a type-II superlattice (system V, dash–dot line). These curves represent an estimate of the minimum linewidth enhancement factor attainable with a DFB structure.

superlattices. The placement of the resonance at 305 meV in one structure rather than 255 meV in the other leads to a 34% reduction of the linewidth enhancement factor at the peak of the gain spectrum. For both systems, the curves shown represent the density at which the linewidth enhancement factor is a minimum. A similar use of intersubband absorption resonances has been used to tailor the index of refraction in a material for the purpose of phase matching.[20]

The discussion to this point has focused on the linewidth enhancement factor at the peak of the gain spectrum. We can estimate the minimum linewidth enhancement factor that can be obtained through detuning of the lasing frequency with a DFB structure by calculating the minimum linewidth enhancement factor over the energy range where the gain is greater than some minimum value. The results for a minimum gain value of 50 cm^{-1} are shown as a function of carrier density in Fig. 4 for systems I, II, and V; the minimum value for each of these curves is listed in Table I. It is possible to obtain linewidth enhancement values as low as 0.3 with the type-II superlattices. This represents a very attractive value for spectrally pure or high power laser operation.

IV. CONCLUSIONS

Linewidth enhancement factors have been calculated for a variety of midinfrared materials. The origin of the smaller linewidth enhancement factors in type-I systems versus bulk systems and in type-II systems versus type-I systems have been identified as better balance between the conduction and valence densities of states and larger conduction miniband dispersion. A new strategy has also been proposed of using intersubband absorption features to tailor the shape of the differential gain spectrum and thus reduce the linewidth enhancement factor.

ACKNOWLEDGMENTS

This research was supported in part by the U.S. Air Force, Air Force Materiel Command, Air Force Research Laboratory, Kirtland AFB, New Mexico, 87117-5777 (Contract No. F29601-97-C0041), and the National Science Foundation (Grant Nos. ECS-9707799 and ECS-9900486).

[1] C. H. Henry, IEEE J. Quantum Electron. **18**, 259 (1982).
[2] F. Kano, Y. Yoshikuni, M. Fukuda, and J. Yoshida, IEEE Photonics Technol. Lett. **3**, 877 (1991); F. Kano, T. Yamanaka, N. Yamamoto, H. Mawatari, Y. Tohmori, and Y. Yoshikuni, IEEE J. Quantum Electron. **30**, 533 (1994).
[3] T. Yamanaka, Y. Yoshikuni, W. Lui, K. Yokoyama, and S. Seki, Appl. Phys. Lett. **62**, 1191 (1993); IEEE J. Quantum Electron. **29**, 1609 (1993).
[4] M. Osinski, Jens Buus, IEEE J. Quantum Electron. **23**, 9 (1987).
[5] S. S. Lee, L. Figueroa, and R. Ramaswamy, IEEE J. Quantum Electron. **25**, 862 (1989).
[6] T. Ohtoshi and N. Chinone, IEEE Photonics Technol. Lett. **1**, 117 (1989).
[7] L. D. Westbrook, Electron. Lett. **21**, 1018 (1985).
[8] J. R. Meyer, C. A. Hoffman, F. J. Bartoli, and L. R. Ram-Mohan, Appl. Phys. Lett. **67**, 757 (1995).
[9] I. Vurgaftman and J. R. Meyer, IEEE J. Sel. Top. Quantum Electron. **3**, 475 (1997).
[10] S. A. Anson, J. T. Olesberg, M. E. Flatté, T. C. Hasenberg, and T. F. Boggess, J. Appl. Phys. **86**, 713 (1999).
[11] J. Faist, F. Capasso, C. Sirtori, D. L. Sivco, A. L. Hutchinson, and A. Y. Cho, Appl. Phys. Lett. **67**, 3057 (1995).
[12] H. K. Choi and G. W. Turner, Appl. Phys. Lett. **67**, 332 (1995).
[13] The structure is taken from Fig. 1 of S. R. Kurtz, A. A. Allerman, and R. M. Biefeld, Appl. Phys. Lett. **70**, 3188 (1997). Values for the strained bulk band gaps and band offsets are taken from the figure.
[14] J. T. Olesberg, M. E. Flatté, B. J. Brown, C. H. Grein, T. C. Hasenberg, S. A. Anson, and T. F. Boggess, Appl. Phys. Lett. **74**, 188 (1999).
[15] M. E. Flatté, C. H. Grein, T. C. Hasenberg, S. A. Anson, D.-J. Jang, J. T. Olesberg, and T. F. Boggess, Phys. Rev. B **59**, 5745 (1999).
[16] J. I. Malin *et al.*, Appl. Phys. Lett. **68**, 2976 (1996).
[17] K. Furuya, Electron. Lett. **21**, 200 (1985).
[18] J. T. Olesberg, S. A. Anson, S. W. McCahon, M. E. Flatté, T. F. Boggess, D. H. Chow, and T. C. Hasenberg, Appl. Phys. Lett. **72**, 229 (1998); D.-J. Jang, Michael E. Flatté, C. H. Grein, J. T. Olesberg, T. C. Hasenberg, and T. F. Boggess, Phys. Rev. B **58**, 13 047 (1998).
[19] The ratio of the zone center masses, $(m_v/m_c)^{3/2}$ (or simply m_v/m_c for the two-dimensional systems), could also be used to quantify the density of states imbalance, but it does not account for the strong nonparabolicity of the valence band or the presence of multiple valence subbands.
[20] G. Almogy, M. Segev, and A. Yariv, Opt. Lett. **19**, 1192 (1994).

Downloaded 19 Jan 2005 to 128.255.34.225. Redistribution subject to AIP license or copyright, see http://jap.aip.org/jap/copyright.jsp